

Accepted Manuscript

Title: A remotely operated drug delivery system with dose control

Author: Ying Yi Jurgen Kosel

PII: S0924-4247(17)30808-7

DOI: <http://dx.doi.org/doi:10.1016/j.sna.2017.05.007>

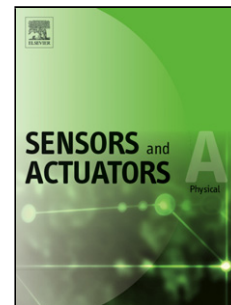
Reference: SNA 10116

To appear in: *Sensors and Actuators A*

Received date: 25-8-2016

Revised date: 21-2-2017

Accepted date: 4-5-2017



Please cite this article as: Y. Yi, J. Kosel, A remotely operated drug delivery system with dose control, *Sensors and Actuators: A Physical* (2017), <http://dx.doi.org/10.1016/j.sna.2017.05.007>

This is a PDF file of an unedited manuscript that has been accepted for publication. As a service to our customers we are providing this early version of the manuscript. The manuscript will undergo copyediting, typesetting, and review of the resulting proof before it is published in its final form. Please note that during the production process errors may be discovered which could affect the content, and all legal disclaimers that apply to the journal pertain.

A remotely operated drug delivery system with dose control

Ying Yi,*^a Jurgen Kosel^b

^aSchool of Engineering, University of British Columbia (UBC), Kelowna, Canada, postal code: V1V 1V7

^bComputer, Electrical and Mathematical Sciences and Engineering (CEMSE) division, King Abdullah University of Science and Technology (KAUST), Thuwal, Saudi Arabia, postal code: 23955-6900.

Email address: * ying.yi@alumni.ubc.ca, phone number: +1-7785817162

“On demand” implantable drug delivery systems can provide optimized treatments, due to their ability to provide targeted, flexible and precise dose release. However, two important issues that need to be carefully considered in a mature device include an effective actuation stimulus and a controllable dose release mechanism. This work focuses on remotely powering an implantable drug delivery system and providing a high degree of control over the released dose. This is accomplished by integration of a resonance-based wireless power transfer system, a constant voltage control circuit and an electrolytic pump. Upon the activation of the wireless power transfer system, the electrolytic actuator is remotely powered by a constant voltage regardless of movements of the device within an effective range of translation and rotation. This in turn contributes to a predictable dose release rate and greater flexibility in the positioning of external powering source. We have conducted proof-of-concept drug delivery studies using the liquid drug in reservoir approach and the solid drug in reservoir approach, respectively. Our experimental results demonstrate that the range of flow rate is mainly determined by the voltage controlled with a Zener diode and the resistance of the implantable device. The latter can be adjusted by connecting different resistors, providing control over the flow rate to meet different clinical needs. The flow rate can be maintained at a constant level within the effective movement range. When using a solid drug substitute with a low solubility, solvent blue 38, the dose release can be kept at 2.36 $\mu\text{g}/\text{cycle}$ within the effective movement range by using an input voltage of 10V_{pp} and a load of 1.5 k Ω , which indicates the feasibility and controllability of our system without any complicated closed-loop sensor.

1. Introduction

Currently, drug therapies are playing an important role for variety of biomedical applications and disease treatments. Conventional modes of drug administration including oral ingestions, eye drops, transdermal delivery and intravenous injections have been widely used¹. However these conventional approaches have limitations in effectively delivering some special drug and new pharmaceutical agents¹, and often cannot optimize the applied medication efficiency²⁻³. Chronic diseases, such as diabetes, usually require frequent injections, which lead to discomfort and trauma to patients. In case of a potent drug, dosing must be precisely controlled within an effective therapeutic concentration range, which is difficult to achieve with conventional drug delivery approaches, frequently leading to overdose induced side effects³⁻⁴.

In contrast to conventional drug delivery methods, recently developed implantable drug delivery systems are very versatile, providing efficient, targeted and controlled dose release. Once the device is implanted, additional surgical operations are not required for a long treatment period (months or even years). This reduces medical cost and patients' discomfort, maintains a desired drug concentration within the therapeutic window³, and improves the therapy's effectiveness. Implantable drug delivery devices are especially advantageous for treating chronic diseases, for example, brain tumors⁵. As the previous studies describe, some of the implants are implemented using polymer materials with biodegradability⁶, sensitivity to pH or temperature⁷, and other characteristics⁸. The delivery carriers include microspheres⁹⁻¹⁰, microcapsules¹¹⁻¹² and hydrogels¹³⁻¹⁴. Most of these works are capable of providing sustained dose releases, however, the actuation mainly comes from diffusion, absorption or osmotic pressure. These devices are “passively controlled”, therefore, dosing is not flexible, and cannot be easily varied based on changing clinical needs.

Over the past two decades, microfabrication technologies have been developed that are able to offer a variety of feasible applications for biological analysis chips¹⁵, tissue engineering¹⁶, and controlled drug delivery¹⁷⁻¹⁸. Different actuation mechanisms have been exploited to trigger drug release by an external stimulus, such as: magnet¹⁹, electromagnetic field²⁰⁻²¹, piezoelectric force²², electrolysis^{4, 23} and so on²⁴, thereby “actively” controlling the dose. Among these actuation mechanisms, the electrolytic actuator has been proven very effective for implantable drug delivery owing to its ability to provide precise flow control, appropriate flow rate, low voltage requirement and little heat generation^{3, 25}. Meng *et al.* optimized the design of their electrolytic pump²³ and used it for delivering liquid drug to the eyeball for treating chronic ocular disease²⁶. Further, DI water was adopted as an electrolyte which can be electrolyzed into oxygen and hydrogen, the generated gases deformed an elastic membrane for delivering the anti-cancer drugs in a mouse study²⁷.

“On demand” controlled implantable drug delivery devices commonly provide a pulsatile dose release, which contribute to a

pulsed-like drug concentration profile³. Therefore, a suitable dose control approach is needed in order to constrain the drug concentration within the therapeutic window and maximize the therapeutic efficacy. More recently, “smart integrated microsystem technologies” have been proposed and indicated the development trend of future implantable drug delivery devices¹. Such advanced drug delivery systems may integrate a micro-actuator with a biosensor²⁸⁻²⁹ or wireless control unit³⁰⁻³¹ or combinations of the above³² in order to monitor the physiological conditions in a patient’s body³³ and release an appropriate amount of drug in accordance with the signals detected³⁴. For example, a telemetry-controlled microchip device that consisted of a wireless communication hardware, power supply, printed circuit boards (PCB) and a drug filled multi-reservoir array was implanted into the subcutaneous tissue of a dog, and remotely programmed to initiate a pulsatile release of the polypeptide leuprolide over 6 months³⁵. However, this versatility comes at a cost of large size and high complexity.

Several attempts have been made towards highly functional and miniature drug delivery systems using efficient microfabrication techniques and simple operation schemes. As demonstrated in^{19, 36}, a magnetic membrane was designed to achieve “on-demand” drug delivery upon the actuation of an external magnetic field. The drug dose released is directly related to the strength of the magnetic field and the duration for which the “magnetic field is turned on”. However, it is difficult to control the dose, since it depends on the distance between the field source and implant, and exposure to a strong magnetic field over an extended period of time raises health concern³⁷⁻³⁸. Inductive coil-based wireless power transfer has superior power transfer efficiency (PTE)³⁹ compared to magnetic force actuation, which was proposed in^{23, 31} for powering ocular drug delivery devices. However, the variation in distance and angle between the implant and the transmission coil will cause varying power levels received after the implantation, thereby resulting in an unpredictable flow rate and dose. Hence, besides the device’s complexity and fabrication cost, the fluctuation of actuator power caused by possible movements need to be addressed in an enhanced implantable drug delivery systems.

In this paper, we introduce a drug delivery system that is easy to fabricate and flexible to operate, combining our previously reported resonance-based wireless power transfer (R-WPT) system, which provides high transfer efficiency⁴⁰, with the low power consumption of an electrolytic pump³. The drug delivery system’s major components, and its delivery performance when directly powered were demonstrated before³, however, we further investigate a remotely powered and controlled scheme using inductive coils herein. As described previously⁴⁰, a small receiver coil (0.5 mm in thickness and 3 cm in diameter), not only saves a considerable amount of space, but also is suitable to be placed under the skin or other flat epidermal organs. In order to mitigate fluctuations of the voltage received, caused by different thicknesses of the tissues of different people and the movements of the wrists and joints, we add a voltage control circuit to regulate the supply voltage of the actuator, rather than adopt a complicated closed-loop sensor. This ensures well-defined drug release rate for a wide range of movements including shifts and rotations between transmitter and receiver. Moreover, different flow rates can be obtained to meet different application needs by changing the resistance of the load before implantation. The released dose can be calculated by multiplying the flow rate and actuation period. This kind of “on demand” release with dose control is suitable for implantable drug delivery systems with specific dose output.

2. Wireless system architecture

The R-WPT technology used for powering the drug delivery device, consists of two parts: the transmitter and the receiver. At the transmitter side, an alternating current (AC) source is applied to the primary coil, creating an AC magnetic field, which induces a voltage across the secondary and load coils at the receiver side. Adopting our previously reported R-WPT system⁴⁰, we further add a constant voltage control circuit at the receiver side. The circuit diagram of this new R-WPT system is illustrated in Fig.1 (a). The resonance frequency of the R-WPT system is 6.7 MHz, following the Industrial, Scientific and Medical radio bands (ISM) standards. Further details of the inductive coils’ structures, inductances, capacitances and resonance frequency are provided elsewhere⁴⁰. The functions of the control circuit include AC/DC conversion and constant voltage supply for driving the actuator. It consists of a 4-diode bridge rectifiers and a 5V Zener diode. The corresponding prototype is illustrated in Fig.1 (b). The Zener diode used in its “reverse bias” mode regulates the voltage output of the rectifier, providing constant 5V, as demonstrated in Supplemental Fig. 1. As a result, the output voltage is constant within an effective transfer distance and rotation angle between transmitter and receiver, both of which can be increased by increasing the input voltage at the transmitter side.

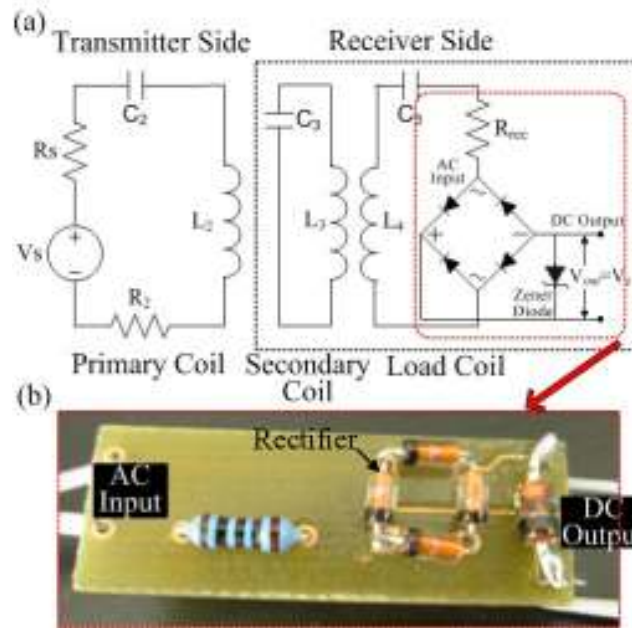


Fig.1 Resonance-based wireless power transfer system with constant voltage control circuit: (a) the circuit model; (b) prototype of the control unit. V_s is the voltage output of the AC power source, R_s is the output impedance, R_{rec} is the resistance of the receiver, C_2 - C_4 denote capacitors, and L_2 - L_4 represent coils.

Besides the voltage applied at the transmitter side, the resistance of the implantable system is another critical parameter that determines the power delivered to the load (PDL)⁴¹. To clarify the relationship between the PDL and the resistance of the load (or drug delivery actuator), an adjustable resistor was connected to the output of the voltage control circuit, and the PDL was measured as a function of transfer distance and resistance value. In this test, the transmitted voltage was fixed at $10V_{pp}$ level. The results shown in Fig. 2 indicate that the optimum load to achieve a maximum PDL varies with the transfer distance. The inset shows that the peak PDL decays with increasing distance, and the optimum load to achieve the peak PDL increases with increasing distance. The impact of the load on the PDL for different distances and rotation angles is demonstrated in Supplemental Fig. 2. It reveals that a higher load resistance improves uniformity of the delivered power for a larger effective distance and rotation range, but at the cost of a reduction of the received power.

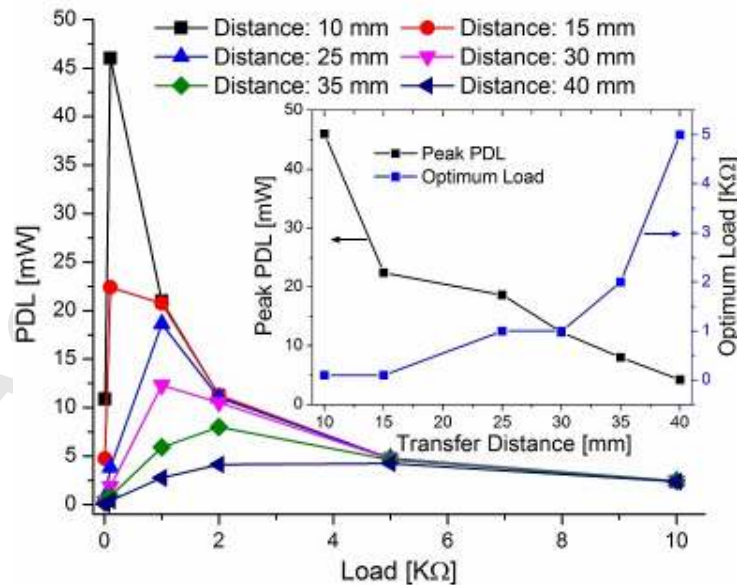


Fig. 2 The power delivered to different loads over different distances.

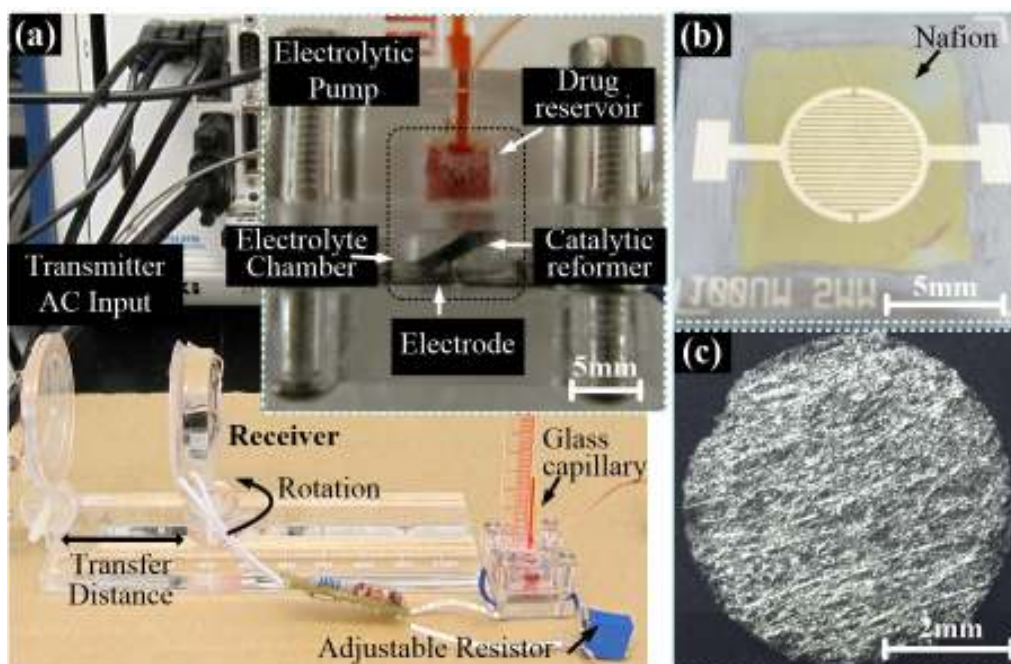


Fig. 3 Photographs of the experimental apparatus with system components. (a) Wirelessly powered drug delivery system with a glass capillary for output measurements. (b) Interdigitated electrodes with Nafion coating. (c) Catalytic reformer.

3. System design and analysis

In this work, we fabricated an electrolytic device for storing and delivering the drug solution. An elastomeric PDMS (poly-dimethylsiloxane) membrane separates the device into two parts: drug reservoir and electrolyte chamber. This diaphragm avoids any interaction between the drug solution and electrolyte, and provides the actuation for driving the drug fluid upon its deflection³. The R-WPT system, voltage control circuit and electrolytic pump were set up in an experimental apparatus as depicted in Fig. 3(a) to investigate the proof of concept drug delivery system. An AC power supply (National Instrument PXI 5402) provides an input voltage of $10V_{pp}$ with a frequency of 6.7 MHz to the transmitter coil, which wirelessly transfers power to the receiver coil. The transfer distance and rotation angle can be adjusted by moving the receiver coil which is electrically connected to the control circuit. After AC to DC conversion and voltage regulation, the output of the control circuit provides a constant voltage for the drug delivery device. An adjustable resistor is electrically connected in series with the pump as the pump alone has a too low resistance³ to maintain a constant voltage. The assembled electrolytic pump is shown in the inset of Fig. 3(a), including the Nafion coated platinum/titanium (Pt/Ti) electrodes (Fig. 3(b)), and a catalytic reformer (Fig. 3(c)), which are both immersed in the electrolyte chamber, the fabrication processes of the electrodes and the catalytic reformer were demonstrated elsewhere^{17, 3}, respectively. The Nafion coating is used to improve the electrolysis efficiency²³, and the catalytic reformer was applied to accelerate bubble recombination within the non-actuation intervals^{3, 20}, thereby reducing the period of delivery for the cyclical actuation mode.

The electrolytic pump's assemble process and working principle were demonstrated previously^{3, 17}. Briefly, once the voltage is received at the electrodes in the electrolytic chamber, the DI water is electrolyzed into hydrogen (H_2) and oxygen (O_2), and the expanding gas deforms the PDMS membrane. This drives the liquid in the reservoir towards the outlet, where it climbs up along the glass capillary, which enables reading the volume of the pumped fluid. Dividing the pumped volume by the time required for pumping yields the flow rate. In this experiment, we used red dyed water as liquid drug substitute. As shown in Fig. 4, increasing the resistance of the connected load, results in a reduced flow rate, which is due to the reduced power received as explained in Fig. 2. On the other hand, an increased resistance allows a constant flow rate to be maintained over a longer separation distance, improving the effective distance range. For example, the pump connected with a load of $500\ \Omega$ can provide an almost constant flow rate of $11\ \mu L/min$ within the effective range of 10 mm to 15 mm, while when increasing the resistance to $1.5\ k\Omega$, the effective distance improves to up to 35mm within which a nominal flow rate of $5\ \mu L/min$ can be maintained. This is because the voltage applied at the pump is kept constant over this effective operation distance, as demonstrated in Supplemental Fig. 2. This result suggests that the flow rate can be "programmed" by choosing a specific load resistor prior to implanting the device, and a compromise needs to be made between effective movement range and achievable flow rate according to the treatment requirements.

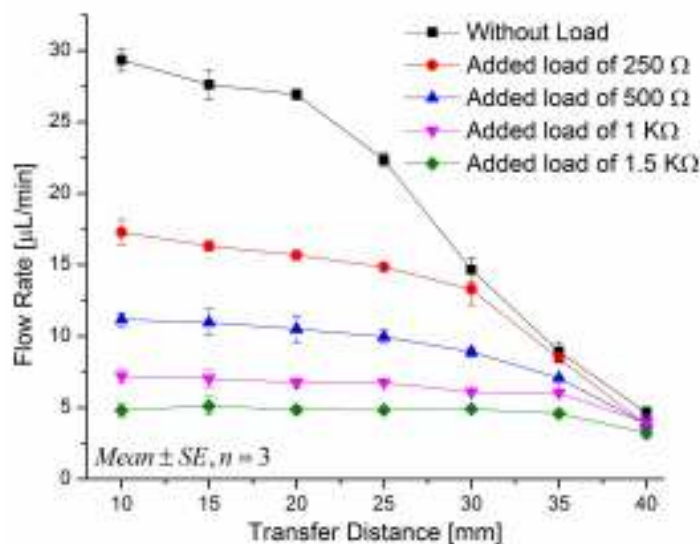


Fig. 4 The flow rate of the electrolytic pump versus the transfer distance for different load resistance values.

Next, we cyclically operated the pump three times with three different conditions: first, the distance between the transmitter coil and receiver coil is 10 mm, and the two coils are co-axially aligned; second, the distance is 25 mm, and the receiver coil is rotated by 30° versus the transmitter coil; third, the distance is 35 mm, and the receiver coil is rotated by 30° versus the transmitter coil. The pump's resistance nonlinearly drops with the increasing applied current, its value ranges from 960Ω to $1.7 \text{ k}\Omega^3$. If the pump is operated with a resistor of low value, for example, a load of 250Ω was used in the experiment. In this case, we can see that the actuation time required for pumping the same volume depends significantly on the different conditions, and the pump's flow rate is sensitive to the movements between transmitter coil and receiver coil as shown in Fig. 5. This is because the total resistance of the load and the pump is too low to obtain a constant voltage in such conditions as explained in Supplemental Fig. 2. Consequently, a constant flow rate cannot be maintained within these movement ranges. On the other hand, when the resistance of the load increases to $1.5 \text{ k}\Omega$, the pump maintains an almost constant flow rate of approximate $5 \mu\text{L}/\text{min}$ within the distance of up to 35 mm and rotation angle of 30° . Thus, the effective movement range has increased in this case, though at a cost of reduced flow rate. These results reveal that our remotely powered device could be capable of achieving a predictable flow rate after implantation despite variation in the operation conditions like distance to and rotation of the implant would exist in practical applications.

The electrolytic reaction is reversible in the presence of Pt^{27} . In our work, within the "power off" intervals, hydrogen and oxygen are gradually recombined to water mainly due to the existence of the Pt coated catalytic reformer in the electrolyte chamber³. The resulting pressure decrease in the electrolyte chamber causes the PDMS membrane to retract back to its original state, thereby drawing the liquid back into the reservoir. The maximum pumped volume at each delivery is limited by the largest deflection of the PDMS membrane. In order to improve the number of delivery cycles within a short testing period, the catalytic reformer is used for accelerating the electrolysis-bubble recombination rate³. In the case of electrolytic actuator-based drug delivery systems, which were using liquid drug in reservoir (LDR) approach^{23, 26-27}, the back flow of fluid caused by the electrolysis-bubble recombination is undesirable, since it dilutes the drug liquid, resulting in unknown dose released over time. Therefore, a variety of valves have been developed to minimize the impact of this issue^{27, 42}. However, when used in combination with a SDR approach, the catalytic reformer can turn this disadvantage into an advantage, because it helps recombine the electrolysis bubbles more rapidly and improves the range of possible drug doses in a given treatment time.

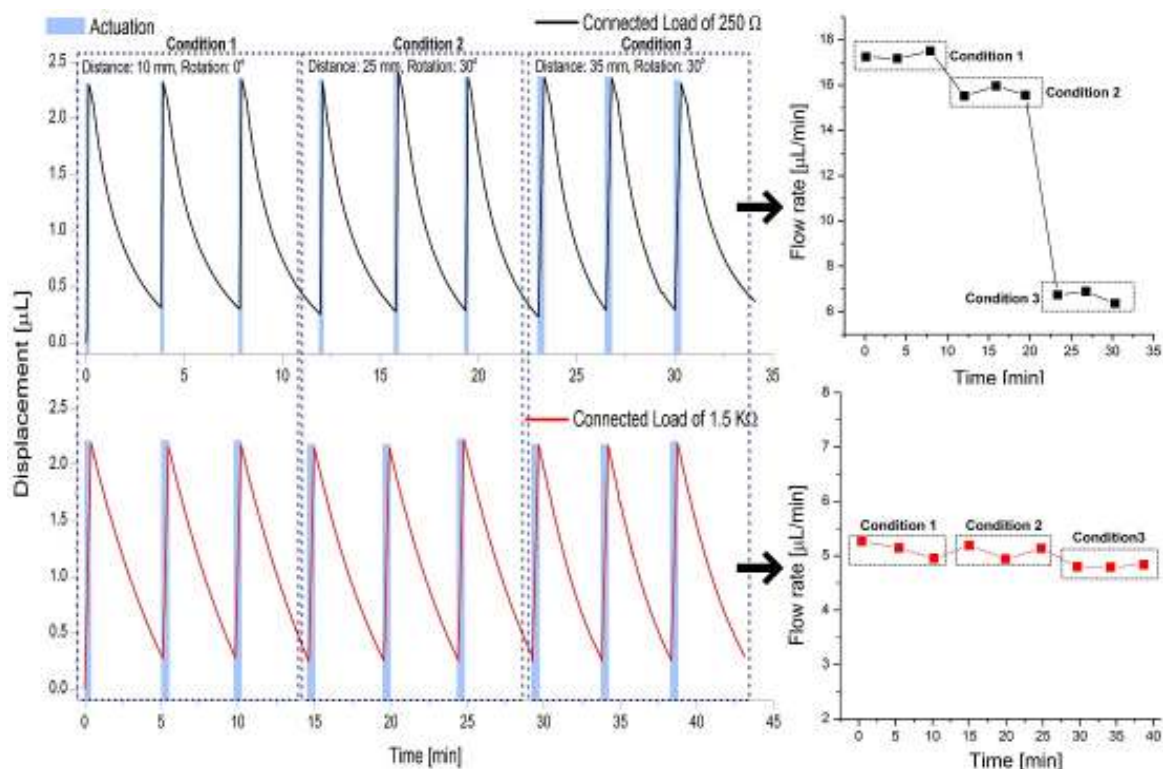


Fig. 5 Periodic pumping pulses of the pump working at different conditions (distance and rotation), showing the impact of the load resistance on the flow rate.

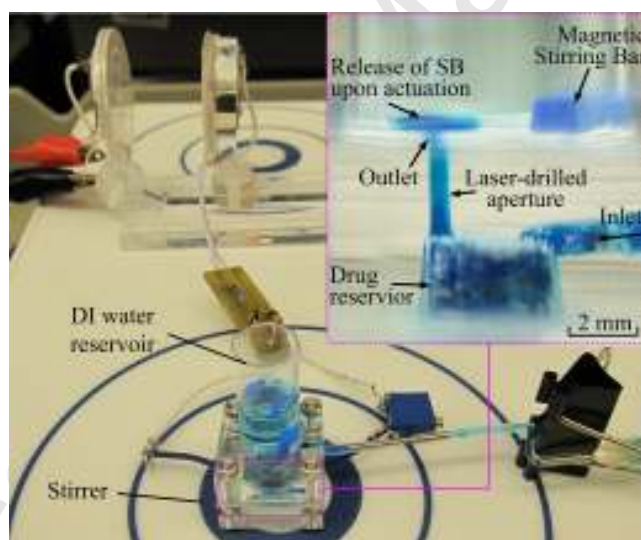


Fig. 6 Experimental apparatus for solid drug delivery, depicting the release of solvent blue 38 into the external liquid upon the electrolytic actuation.

4. Cyclically operated solid drug delivery system

For the applications of hydrophobic drugs, for example, docetaxel (solubility of $2.5 \mu\text{g/L}$ in water), the LDR approach cannot provide an effective solution for implantable drug delivery, due to the large volume required to store useful quantities of active ingredient. An alternative approach is to store the drug in its solid-form. In case of the SDR approach, small amounts of the stored solid drug are repeatedly dissolved into body fluid⁴³, maintaining a reproducible concentration of drug solution over an extended period of time (several months or years). The design of our electrolytic pump with the added catalytic reformer provides a suitable platform for such cyclic operation³. In this work, we use solvent blue 38 as a substitute for the solid drug, owing to its low solubility in water and its solid-form can be maintained in the reservoir for a large number of operation cycles.

The experimental apparatus depicted in Fig. 6 is set up to evaluate the SDR device's dose release performance. Briefly, solvent blue 38 is partially dissolved in the drug reservoir. Another reservoir filled with DI water is placed at the outlet of the pump to which the dissolved drug solution is delivered (see the inset of Fig. 6). The device is put on a stirrer (Advanced Multiposition Stirrer, Henry Troemner LLC, USA), and a magnetic stirring bar immersed in the external reservoir helps to uniformly disperse the delivered solution in the external liquid. In this idealized testing environment, cell absorption and naturally occurring flow rates in the body are not taken into account. The concentration change of the external liquid is detected by microliter spectrophotometry (Picodrop Ltd., UK) at the end of each delivery, so that the dose released upon each actuation is measured. A load resistor of 1.5 k Ω connected to the electrolytic pump was used, to obtain a constant amount of drug release for the different movement conditions.

Firstly, the setup was used to verify the two events in the cyclical operation of the SDR system: 1) pumping the dissolved drug solution during the “power on” period, and 2) automatically refilling the drug reservoir within the “power off” period. The experiment was conducted, with an input voltage of 10 V_{pp}, and a separation distance of 10 mm between the transmitter coil and receiver coil, which were co-axially aligned. The series of images in Fig. 7 shows one cycle of “power on and off”, verifying these two events involved in a cyclically operated SDR drug delivery process: the electrolytic pump is wirelessly powered, and driving the drug solution out of the reservoir; refilling is caused by electrolysis-bubble recombination, which draws liquid back into the reservoir to mix with the remaining drug solution. Solid drug dissolves into mixture until the reservoir once again reaches the solubility limit of the drug. Note that the pumping rate of the drug delivery device must be consistent with or less than naturally occurring flow rates in the body, especially when this cyclical actuation mechanism is applied. Therefore, the released drug can diffuse away from the delivery site before it is sucked back into the reservoir during the refilling stage.

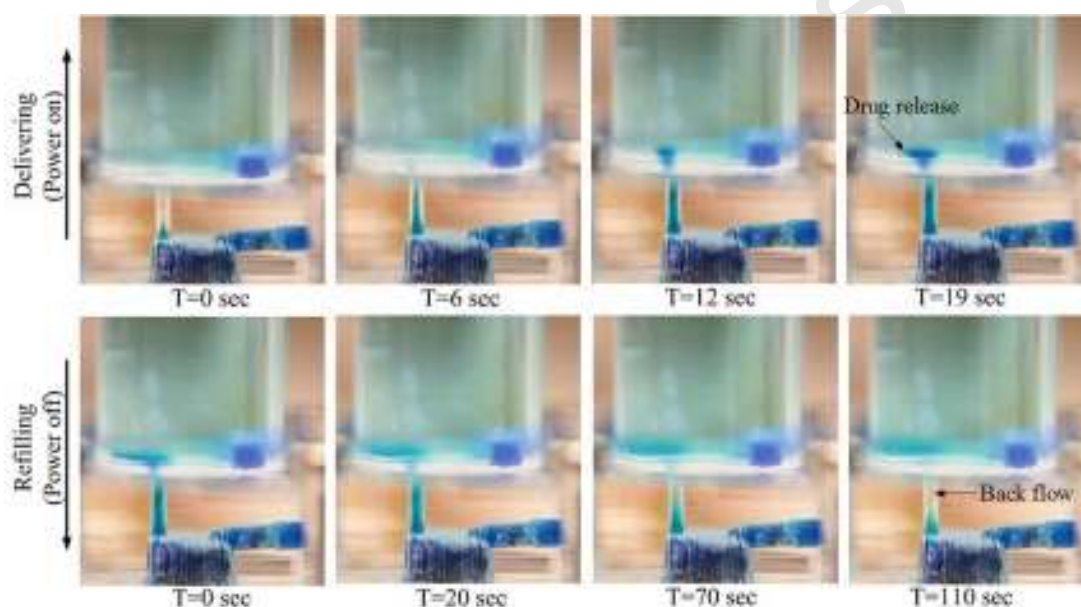


Fig. 7 Microscope images of one cycle of drug delivery process under “power on and off” operation, illustrating the reversibility of the fluid upon the PDMS membrane’s deflection.

Next, we studied the effect of distance between and alignment of the transmitter and receiver coils on the release behaviour, applying the same conditions as stated in Fig. 5. In each condition, the device was cyclically operated “power on and off” for 3 times, with a “power on” time of 0.5 minute and a “power off” time of 5.5 minutes, which is sufficient for fully recombining the electrolysis-bubbles³. The measured dose released at each delivery cycle is shown in Fig. 8. As expected, the dose in each condition keeps almost constant with an average dose value of 2.36 $\mu\text{g}/\text{cycle}$, due to a stable flow rate achieved within the effective range of distance and orientation. This also indicates a stable drug concentration, which is due to the concentration of the pumped drug solution remaining close to the drug’s maximum solubility³. In this experiment, an average dose of 2.36 $\mu\text{g}/\text{cycle}$ can be maintained within the effective range of distance and orientation, for example, the effective transfer distance of 35 mm and rotation angle of 30° is presented for the chosen experimental parameters. Within the effective range, our R-WPT system with an addition of a constant voltage control circuit can remotely power the electrolysis based drug delivery device and provide a well-defined release rate, thereby controlling the drug dose without feedback from the device based only on the actuation period.

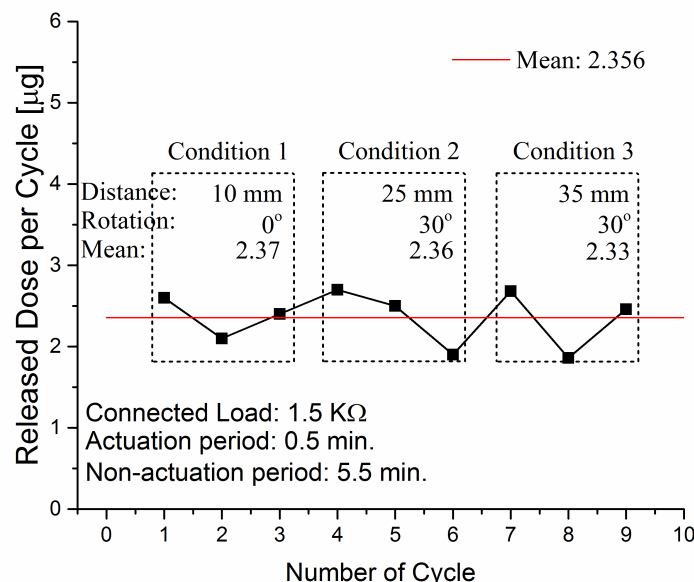


Fig. 8 The dose of released drug per actuation for different distances between the transmitter and receiver coils as well as different rotation angles.

5. Conclusions

Implantable drug delivery systems have advantages in medical treatments that require frequent drug therapies and precise dose control. This work presents a proof of concept electrolytic pump drug delivery system that is remotely powered and controlled by a combination of a highly efficient resonant wireless power transfer system and a constant voltage control circuit. This combination allows consistent open-loop control of the dosage based on actuation time alone, even with inconsistent placement of the transmission coil with respect to the receiving coil of the device, as expected in real life application. The results show the feasibility of such a system for controlling the release rate and dosage with high precision within a given movement range. The proposed simple circuit design regulates the voltage applied to the electrolytic pump regardless of the distance and rotation between the transmitter and receiver coils within the effective movement range, leading to a well-defined flow rate released in the LDR device. The effective movement range can be easily modified via the input voltage at transmitter side or via an electric load resistor at the receiver side. Similarly, the flow rate can be adjusted to meet different clinical needs by connecting different load resistors to the receiver side. The experimental analysis also shows that by using a smaller load resistor, the flow rate can be increased but at a cost of higher sensitivity to shift and rotation between the transmitter and receiver, and increasing the resistance enlarges the effective movement range. The SDR approach has also been evaluated for our system, and for the chosen experimental parameters, a constant dose of 2.36 µg at each delivery cycle is maintained within the effective movement range of 35 mm and 30°.

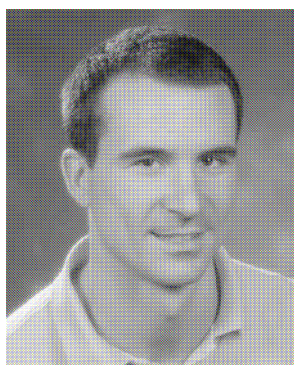
References

- [1]. S.Z. Razzacki, P.K. Thwar, M. Yang, V.M. Ugaz, M.A. Burns, "Integrated Microsystems for controlled drug delivery," *Adv. Drug Deliv. Rev.*, 56 (2), pp. 185–198, 2004.
- [2]. D. C. Metrikin, R. Anand, "Intravitreal drug administration with depot devices," *Current opinion in ophthalmology*, 5(3), pp. 21-29, 1994.
- [3]. Y. Yi, U. Buttner, I. G. Foulds, "A cyclically actuated electrolytic drug delivery device," *Lab on a Chip*, 15, pp. 3540–3548, 2015.
- [4]. E. Meng, T. Hoang, "MEMS-enabled implantable drug infusion pumps for laboratory animal research, preclinical, and clinical applications," *Advanced drug delivery reviews*, 64(14), pp. 1628-1638, 2012.
- [5]. Y. Li, H. L. H. Duc, B. Tyler, T. Williams, M. Tupper, R. Langer, and M. J. Cima, "In vivo delivery of BCNU from a MEMS device to a tumor model," *J. Controlled Release*, 106(1), pp. 138–145, 2005.
- [6]. A. Göpferich, "Mechanisms of polymer degradation and erosion," *Biomaterials*, 17(2), pp.103-114, 1996.
- [7]. R. Yoshida, "Design of functional polymer gels and their application to biomimetic materials," *Current Organic Chemistry*, 9(16), pp.1617-1641, 2005.
- [8]. K. E. Uhrich, S. M. Cannizzaro, R. S. Langer, K. M. Shakesheff, "Polymeric systems for controlled drug release," *Chemical reviews*, 99(11), pp. 3181-3198, 1999.
- [9]. W. Wei, L. Yuan, G. Hu, L. Y. Wang, J. Wu, X. Hu, Z. G. Su, and G. H. Ma, "Monodisperse chitosan microspheres with interesting structures for protein drug delivery," *Adv Mater.*, 20(12), pp. 2292-2296, 2008.
- [10]. I. Yuki, M. Matsusaki, T. Kida, and M. Akashi, "Locally controlled release of basic fibroblast growth factor from multilayered capsules," *Biomacromolecules*, 9(8), pp. 2202-2206, 2008.
- [11]. H. M. Chen, R. C. MacDonald, S. Li, N. L. Krett, S. T. Rosen, and T. V. O'Halloran, "Lipid encapsulation of arsenic trioxide attenuates cytotoxicity and allows for controlled anticancer drug release." *Journal of the American Chemical Society*, 128(41), pp. 13348-13349, 2006.

- [12]. G. De, G. Bruno, etc. "Intracellularly degradable polyelectrolyte microcapsules," *Advanced materials*, 18(8), pp. 1005-1009, 2006.
- [13]. N. S. Satarkar, and J. Zach Hilt, "Magnetic hydrogel nanocomposites for remote controlled pulsatile drug release," *Journal of Controlled Release*, 130(3), pp. 246-251, 2008.
- [14]. P. D. Thornton, R. J. Mart, and R. V. Ulijn, "Enzyme-Responsive Polymer Hydrogel Particles for Controlled Release," *Advanced materials*, 19(9), pp. 1252-1256, 2007.
- [15]. D. J. Laser, J. G. Santiago, "A review of micropumps," *Journal of micromechanics and microengineering*, 14(6), pp. 35-64, 2004.
- [16]. W. M. Saltzman, and W. L. Olbricht, "Building drug delivery into tissue engineering design," *Nature Reviews Drug Discovery*, 1(3), pp. 177-186, 2002.
- [17]. Yi, Y., Buttner, U., Carreno, A. A., Conchouso, D., & Foulds, I. G., "A pulsed mode electrolytic drug delivery device," *Journal of Micromechanics and Microengineering*, 25(10), pp. 105011, 2015.
- [18]. B. Ziaie, A. Baldi, M. Lei, Y. Gu, and R. A. Siegel, "Hard and soft micromachining for BioMEMS: review of techniques and examples of applications in microfluidics and drug delivery," *Advanced drug delivery reviews*, 56(2), pp. 145-172, 2004.
- [19]. F. N. Pirmoradi, J. K. Jackson, H. M. Burt and M. Chiao, "A magnetically controlled MEMS device for drug delivery: design, fabrication, and testing," *Lab on a Chip*, 11(18), pp. 3072-3080, 2011.
- [20]. Y. Yi, A. Zaher, O. Yassine, J. Kosel, Ian G. Foulds, "A remotely operated drug delivery system with an electrolytic pump and a thermo-responsive valve," *Biomicrofluidics*, 9(5), pp. 052608, 2015.
- [21]. K. Cai, Z. Luo, Y. Hu, X. Chen, Y. Liao, L. Yang, and L. Deng, "Magnetically triggered reversible controlled drug delivery from microfabricated polymeric multireservoir devices," *Adv. Mater.*, 21, pp. 4045-4049, 2009.
- [22]. J. Kan, Z. Yang, T. J. Peng, G. M. Cheng, and B. Wu, "Design and test of a high-performance piezoelectric micropump for drug delivery," *Sensors and Actuators A: Physical*, 121(1), pp. 156-161, 2005.
- [23]. P. Y. Li, R. Sheybani, C. A. Gutierrez, J. T. W. Kuo and E. Meng, "A parylene bellows electrochemical actuator," *Journal of Microelectromechanical Systems*, 19(1), pp. 215-228, 2010.
- [24]. A. Nisar, A. Nitin, B. Mahaisvariya, and A. Tuantranont, "MEMS-based micropumps in drug delivery and biomedical applications," *Sensors and Actuators B: Chemical*, 130(2), pp. 917-942, 2008.
- [25]. D. A. Ateya, A. A. Shah, and S. Z. Hua, "An electrolytically actuated micropump," *Review of scientific instruments*, 75(4), pp. 915-920, 2004.
- [26]. P. Y. Li, J. Shih, R. Lo, S. Saati, R. Agrawal, M. S. Humayun, Y. C. Tai and E. Meng, "An electrochemical intraocular drug delivery device," *Sensors and Actuators A: Physical*, 143(1), pp. 41-48, 2008.
- [27]. H. Gensler, R. Sheybani, P. Y. Li, R. L. Mann and E. Meng, "An implantable MEMS micropump system for drug delivery in small animals," *Biomedical microdevices*, 14(3), pp. 483-496, 2012.
- [28]. M. Ngoepe, Y. E. Choonara, C. Tyagi, L. K. Tomar, L. C. D. Toit, P. Kumar, V. M. Ndesendo, and V. Pillay, "Integration of biosensors and drug delivery technologies for early detection and chronic management of illness," *Sensors*, 13(6), pp. 7680-7713, 2013.
- [29]. A. C. Grayson, R. S. Richards, A. M. Johnson, N. T. Flynn, Y. Li, M. J. Cima, and R. Langer, "A BioMEMS review: MEMS technology for physiologically integrated devices," *Proceedings of the IEEE*, 92(1), pp. 6-21, 2004.
- [30]. S. Rahimi, E. H. Sarraf, G. K. Wong, and K. Takahata, "Implantable drug delivery device using frequency-controlled wireless hydrogel microvalves," *Biomedical microdevices*, 13(2), pp. 267-277, 2011.
- [31]. T. B. Tang, S. Smith, B. W. Flynn, J. T. M. Stevenson, A. M. Gundlach, H. M. Reekie, A. J. Walton, "Implementation of wireless power transfer and communications for an implantable ocular drug delivery system," *IET Nanobiotechnology*, 2(3), pp. 72-79, 2008.
- [32]. Sheybani, R., Cobo, A., & Meng, E. (2015). Wireless programmable electrochemical drug delivery micropump with fully integrated electrochemical dosing sensors. *Biomedical microdevices*, 17(4), 1-13.
- [33]. H. K. A. Tsai, E. A. Moschou, S. Daunert, M. Madou, and L. Kulinsky, "Integrating Biosensors and Drug Delivery: A Step Closer Toward Scalable Responsive Drug-Delivery Systems," *Advanced Materials*, 21(6), pp. 656-660, 2009.
- [34]. M. Privman, T. K. Tam, V. Bocharova, H. Jan, J. Wang, and E. Katz, "Responsive interface switchable by logically processed physiological signals: Toward "smart" actuators for signal amplification and drug delivery," *ACS applied materials & interfaces*, 3(5), pp. 1620-1623, 2011.
- [35]. J. H. Prescott, S. Lipka, S. Baldwin, N. F. Sheppard, J. M. Maloney, J. Coppeta, B. Yomtov, M. A. Staples and J. T. Santini, "Chronic, programmed polypeptide delivery from an implanted, multireservoir microchip device," *Nature biotechnology*, 24(4), pp. 437-438, 2006.
- [36]. T. Hoare, J. Santamaria, G. F. Goya, S. Irusta, D. Lin, S. Lau, D.S. Kohane, "A magnetically triggered composite membrane for on-demand drug delivery," *Nano letters*, 9(10), pp. 3651-3657, 2009.
- [37]. J. Miyakoshi, M. Yoshida, K. Shibuya, & M. Hiraoka, "Exposure to strong magnetic fields at power frequency potentiates X-ray-induced DNA strand breaks," *Journal of radiation research*, 41(3), 293-302, 2000.
- [38]. H. Lai, & N. P. Singh, "Magnetic-field-induced DNA strand breaks in brain cells of the rat," *Environmental Health Perspectives*, 112(6), 687, 2004.
- [39]. A. K. RamRakhyani, S. Mirabbasi, and M. Chiao, "Design and optimization of resonance-based efficient wireless power delivery systems for biomedical implants," *IEEE Transactions on Biomedical Circuits and Systems*, 5(1), pp. 48-63, 2011.
- [40]. Yi, Y., Buttner, U., Fan, Y., & Foulds, I. G., "Design and optimization of a 3-coil resonance-based wireless power transfer system for biomedical implants," *International Journal of Circuit Theory and Applications*, 43(10), pp. 1379-1390, 2015.
- [41]. M. Kiani, U.-M. Jow, and M. Ghovanloo, "Design and optimization of a 3-coil inductive link for efficient wireless power transmission," *IEEE Transactions on Biomedical Circuits and Systems*, 5(6), pp. 579-591, 2011.
- [42]. R. Lo, & E. Meng, "A modular heat-shrink-packaged check valve with high pressure shutoff," *Journal of Microelectromechanical Systems*, 20(5), pp. 1163-1173, 2011.
- [43]. F. N. Pirmoradi, J. K. Jackson, H. M. Burt and M. Chiao, "On-demand controlled release of docetaxel from a battery-less MEMS drug delivery device," *Lab on a Chip*, 11(16), pp. 2744-2752, 2011.



Ying Yi received the B.S degree in Information Technology from HeBei Normal University, in HeBei Province, China, and M.Eng. degrees from the Department of Electronics and Radio Engineering, Kyung Hee University, Korea, in 2008 and 2010, respectively. In 2012, he started the Ph.d program at the King Abdullah University of Science and Technology, Saudi Arabia, and received the Ph.d degree from the University of British Columbia, Canada, in 2016. Since 2016 July, he joined the Microsystems and Nanotechnology Research Group at The University of British Columbia as a Post-Doctoral Fellow. His current research areas include microfluidics, Lab-on-a-Chip, and BioMEMS.



Jürgen Kosel received the Dipl.-Ing.(M.Sc.) and D.Sc. degrees in electrical engineering from the Vienna University of Technology, Vienna, Austria, in 2002 and 2006, respectively. He was a Post-Doctoral Fellow with the Biomedical Engineering Research Group, Stellenbosch University, Stellenbosch, South Africa, from 2007 to 2009. From 2006 to 2007, he was a Project Manager with the automotive industry, Magna Powertrain, Graz, Austria. He has been an assistant professor of Electrical Engineering with the King Abdullah University of Science and Technology (KAUST), Thuwal, Saudi Arabia, from 2009 to 2015. Since 2015 he is Associate Professor at KAUST, where he is currently with the Computer, Electrical and Mathematical Sciences and Engineering Division, and principal investigator of the Sensing, Magnetism and Microsystems Research Group. His research interests include micro- and nano transducers.